Evaluation of Global Reanalysis Land Surface Wind Speed Trends to Support Wind Energy Development Using In Situ Observations

WENXIN FAN,[a] YI LIU,[a] ADRIAN CHAPPELL,[b] LI DONG,[c] RONGRONG XU,[a] MARIE EKSTRÖM,[b] TZUNG-MAY FU,[a] AND ZHENZHONG ZENG[a]

[a] *School of Environmental Science and Engineering, Southern University of Science and Technology, Shenzhen, China*
[b] *School of Earth and Ocean Sciences, Cardiff University, Cardiff, United Kingdom*
[c] *Department of Earth and Space Science, Southern University of Science and Technology, Shenzhen, China*

(Manuscript received 19 February 2020, in final form 14 October 2020)

ABSTRACT: Global reanalysis products are important tools across disciplines to study past meteorological changes and are especially useful for wind energy resource evaluations. Studies of observed wind speed show that land surface wind speed declined globally since the 1960s (known as global terrestrial stilling) but reversed with a turning point around 2010. Whether the declining trend and the turning point have been captured by reanalysis products remains unknown so far. To fill this research gap, a systematic assessment of climatological winds and trends in five reanalysis products (ERA5, ERA-Interim, MERRA-2, JRA-55, and CFSv2) was conducted by comparing gridcell time series of 10-m wind speed with observational data from 1439 in situ meteorological stations for the period 1989–2018. Overall, ERA5 is the closest to the observations according to the evaluation of climatological winds. However, substantial discrepancies were found between observations and simulated wind speeds. No reanalysis product showed similar change to that of the global observations, although some showed regional agreement. This discrepancy between observed and reanalysis land surface wind speed indicates the need for prudence when using reanalysis products for the evaluation and prediction of winds. The possible reasons for the inconsistent wind speed trends between reanalysis products and observations are analyzed. The results show that wind energy production should select different products for different regions to minimize the discrepancy with observations.

KEYWORDS: Wind; Surface observations; Reanalysis data; Renewable energy

1. Introduction

Wind power plays an important role in transforming global energy systems toward low carbon emission renewable systems. Because wind energy density is proportional to the cube of wind speed, even small changes to wind speed at the height of a turbine hub can greatly impact wind power generation and overall economy of wind energy companies (Lu et al. 2009). Hence, understanding regional wind speed trends and variability is critical when optimizing wind turbines and wind power industry investments (Veers et al. 2019). Because of the lack of long-term and homogenous historical wind speed observations, wind energy operators often utilize reanalysis products to evaluate wind speed changes. However, land surface wind speed changes from these products are associated with large uncertainties, originating from, for example, model inadequacies and spatiotemporal distribution of assimilated observation data (Rose and Apt 2016; Wen et al. 2019). Therefore, it is critical to evaluate the changes in magnitude, trend, and variability of land surface wind speed in global reanalysis products relative to in situ observations that record the actual wind speed.

Many studies have shown that global land surface wind speed has been declining significantly since the 1960s, especially over Northern Hemisphere midlatitude regions (McVicar et al. 2012; Vautard et al. 2010; Wu et al. 2018). This phenomenon is termed global terrestrial stilling (Roderick et al. 2007). Recently, Zeng et al. (2019) found that the trend in global land surface wind speed reversed around 2010 with rapidly increased trend beginning in the following year, especially in North America, Europe, and Asia. Regionally, surface wind speed has increased since 1998 in Tehran, Iran (Keyhani et al. 2010), since 2000 in eastern China (Zha et al. 2019), and since 2003 in South Korea (Kim and Paik 2015). Whether these trends in observed station data are captured in global reanalysis products has not yet been evaluated. Such evaluation is critical and urgent given the wide application of reanalysis products in wind resource evaluations (Carvalho et al. 2014), hydrology simulation (Siam et al. 2013), land surface modeling (Sheffield et al. 2006), and environmental impact assessment (Marsh et al. 2007). For example, for dust emission models (Menut 2008) and evaporation models (Hobbins et al. 2012), surface wind speed is one of the most important driving factors.

Other studies have evaluated the uncertainties of wind speed trends in reanalysis products. Torralba et al. (2017) used three reanalysis products (ERA-Interim, MERRA-2, and JRA-55) to evaluate global wind speed trend during 1980–2015. They found an increasing trend over oceans and decreasing trend over lands. Yet the decreasing trends over land differed significantly among reanalysis products, which was also found in other reanalysis comparisons among the European Centre for Medium-Range Weather Forecasts (ECMWF) twentieth-century reanalysis (ERA-20C), 10-member ensemble of coupled climate reanalyses of the twentieth century (CERA-20C), and the "model only" ERA-20C (ERA-20CM)

Corresponding author: Zhenzhong Zeng, zengzz@sustech.edu.cn

DOI: 10.1175/JAMC-D-20-0037.1

(Wohland et al. 2019). Notably, these studies did not verify modeled trends with observed data, hampering the assessment of fidelity relative to observed wind speed trends. Similarly, Ramon et al. (2019) analyzed wind speed trends in five global reanalysis products for the period 1980 to 2017 [ERA5, ERA-Interim, JRA-55, MERRA-2, and National Centers for Environmental Prediction–National Center for Atmospheric Research (NCEP–NCAR) R1]. They found specific differences in these products for average wind speed, annual variation, and long-term trend of wind speed characteristics, especially for land surface wind speed. However, like most of the wind speed trend studies, they only focused on the overall decreasing wind speed trend over land, neglecting the fact that the decreasing trend has reversed recently.

While existing research has focused on the intercomparison of reanalysis products, our study aims to determine which reanalysis products reproduce the trends and variabilities in observed wind data. We investigated both overall trend and piecewise trends over land areas in recent decades. The motivation of this work is that closer agreement of reanalysis products with observed data supports that the products are more appropriate for both meteorology and wind energy related research such as wind turbine optimization. Here we focus on the period 1989–2018 to capture the reported global decrease and recent reversal of wind speed trends. Reanalysis wind speeds are represented by five well-documented global products (see section 2a) and observed data is sourced from the global subdaily station dataset Hadley Integrated Surface Database (HadISD) (Dunn et al. 2016). Using only stations with homogenous records, 1439 stations were selected from a total of 8139 stations.

Wind speed trends have the most direct and significant impacts on the development of the wind power industry. The magnitude of wind speed is of significance. Thus, we first evaluated the climatological winds of reanalysis products to select the reanalysis products closer to the observed wind speed with regard to the multiyear average performance. The trend in wind speed is also important. If the global terrestrial stilling continues, available wind resources will decrease with the reduced wind speeds. The reduction will impact the wind power industry negatively, while an increase in speeds can play a positive role in the wind power industry, along with environmental, economic, and scientific impacts. To better characterize the wind energy potential, we also evaluated the wind speed frequency distribution. Because reanalysis products are often used to predict wind energy production in recent years, we quantify and compare the potential changes in wind energy after the turning point.

2. Datasets and methods

a. Global reanalysis products

Reanalysis 10-m winds are obtained from four different institutions, including ERA5 (Hersbach and Dee 2016) and ERA-Interim (Dee et al. 2011) from ECMWF; the Japanese 55-year Reanalysis (Kobayashi et al. 2015) from the Japan Meteorological Agency (JMA); the Modern-Era Retrospective Analysis for Research and Applications, version 2 (Gelaro et al. 2017), from NASA Goddard Earth Sciences Data and Information Services Center (GES DISC); and Climate Forecast System, version 2 (Saha et al. 2014), from NCEP. The full name, institution, period covered, assimilation system, output frequency, spatial resolution, assimilation data type, and URL are summarized in Table 1. These represent state-of-the art reanalysis products that are often used to evaluate wind energy resources. For each dataset, the gridcell time series (1989–2018) for each selected HadISD station (Fig. 2) was selected for analysis.

ERA5 (Hersbach and Dee 2016) is the fifth-generation ECMWF reanalysis product replacing ERA-Interim and is currently being extended back to 1950 (expected completion in 2020). ERA5 assimilate many observational data with 4D-Var in CY41R2 of ECMWF's Integrated Forecast System (IFS). The model output at hourly frequency with a T639 triangular truncation of spectral coefficients. The data have a horizontal resolution of 31 km (0.281 25°; all resolutions are representative for the equator) and 137 hybrid levels in the vertical direction, with the top level at 1 Pa. ERA5 assimilates the data from ships, buoys, aircraft records, radiosonde profiles, QuikSCAT, *ERS-1*, *ERS-2*, and SSM/I. In addition, ERA5 also assimilates various newly reprocessed datasets and recent instruments that could not be ingested in ERA-Interim.

ERA-Interim (Dee et al. 2011) is the predecessor of ERA5. Its assimilation system is based on the IFS (Cy31r2) with a 4D-Var scheme. This dataset begins in 1979 and ends on 31 August 2019 when it was superseded by ERA5. ERA-Interim is available on a 6-hourly temporal resolution and a T255 spectral truncation (0.75°, or ~79 km), with 60 vertical levels. ERA-Interim assimilated the same data types as ERA5.

JRA-55 (Kobayashi et al. 2015) is based on JMA's operational system with a 4D-Var data assimilation scheme as of December 2009. The product begins in 1958 and is ongoing; hence it has the greatest temporal extent of the considered datasets. Data are available on 6-hourly resolution with a T369 spectral truncation, a horizontal resolution of 55 km (0.562°), and 60 vertical levels. In addition to the conventional inputs, it also assimilates the ASCAT ocean surface winds.

MERRA-2 (Gelaro et al. 2017) is the successor of MERRA. It is an atmospheric reanalysis using the Goddard Earth Observing System Model, version 5 (GEOS-5), with Atmospheric Data Assimilation System (ADAS). MERRA-2 covers the period from 1980 to the present, continuing as an ongoing climate reanalysis product. This dataset has an hourly temporal resolution and spatial resolution of 0.5° × 0.625° (about 55 km). MERRA-2 has the most data types for assimilation, including NRL WindSat and ASCAT ocean surface winds (Table 1).

CFSv2 (Saha et al. 2014) is a fully coupled ocean–land–atmosphere system for seasonal forecasts, implemented at NCEP in April 2011. The atmospheric part of CFSv2 adopts the Global Forecast System (GFS), with a spatial resolution of T126L64 (0.937°, or ~100 km) and a vertical resolution of 64 levels. CFSv2 provides reforecast simulations to evaluate and calibrate model simulations. CFSv2 data include retrospective

TABLE 1. A summary of the main characteristics of the global reanalysis evaluated in this study.

	ERA5	ERA-I	JRA-55	MERRA-2	CFSv2
Full name	ECMWF Fifth Major Global Reanalysis	ECMWF interim reanalysis (ERA-Interim)	Japanese 55-year Reanalysis	Modern-Era Retrospective analysis for Research and Applications, version 2	Climate Forecast System, version 2
Institution	ECMWF	ECMWF	JMA	NASA	NCEP
Period covered	1950–present	1979–present	1958–present	1980–present	2011–present
Assimilation system	IFS Cycle 41r2 4D-Var	IFS Cycle 31r2 4D-Var	JMA's operational system 4D-Var	GEOS-5 and ADAS 3D-Var	Global Data Assimilation System 3D-VAR
Output frequency	1 hourly	6 hourly	6 hourly	1 hourly	6 hourly
Spatial resolution	31 km (TL639); 137 levels to 1 Pa	79 km (TL255); 60 levels to 10 Pa	55 km (TL319); 60 levels to 10 Pa	50 km (0.5° × 0.625°); 72 levels to 1 Pa	100 km (TL126); 64 levels to 26 Pa
Assimilation data type	Ships, buoys, aircraft records, radiosonde profiles, QuikSCAT, *ERS-1*, *ERS-2*, and SSM/I	Ships, buoys, aircraft records, radiosonde profiles, QuikSCAT, *ERS-1*, *ERS-2*, and SSM/I	ships, buoys, aircraft records, radiosonde profiles, QuikSCAT, *ERS-1*, *ERS-2*, SSM/I, and ASCAT	Ships, buoys, aircraft records, radiosonde profiles, QuikSCAT, *ERS-1*, *ERS-2*, SSM/I, NRL WindSat, and ASCAT	Ships, buoys, aircraft records, radiosonde profiles, QuikSCAT, *ERS-1*, *ERS-2*, SSM/I, and NRL WindSat
URL	https://www.ecmwf.int/en/forecasts/datasets/reanalysis-datasets/era5	https://www.ecmwf.int/en/forecasts/datasets/reanalysis-datasets/era-interim	https://jra.kishou.go.jp/JRA-55/index_ja.html	https://disc.gsfc.nasa.gov/datasets/M2IMNXLFO_5.12.4/summary?keywords=%22MERRA-2%22	https://www.ncdc.noaa.gov/data-access/model-data/model-datasets/climate-forecast-system-version2-cfsv2

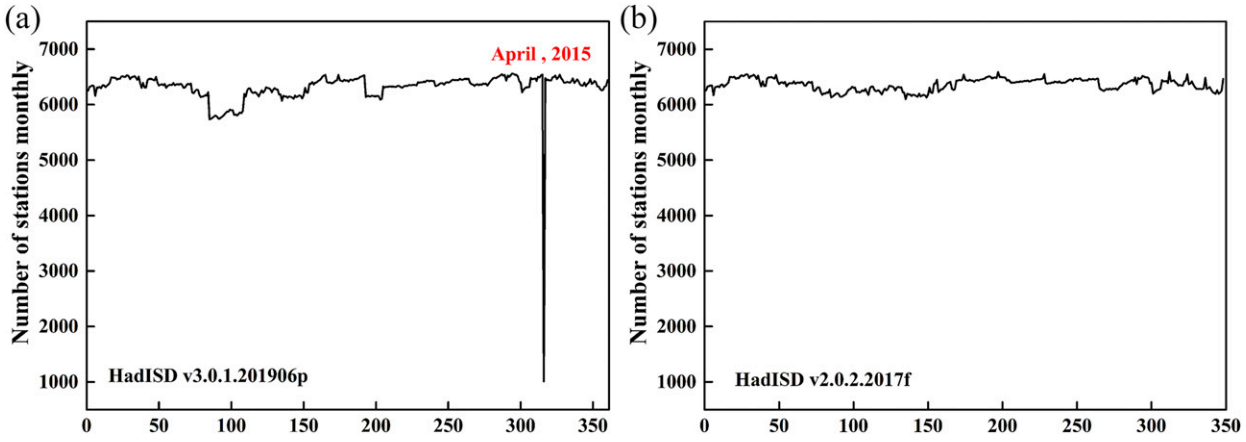

FIG. 1. Number of stations by month in two HadISD versions: (a) v3.0 for 1989–2018 and (b) v2.0 for 1989–2017.

forecasts from January 1982 to March 2011 and real-time forecasts after April 2011. Given the different configurations of the two predictions, the reforecast datasets were used in this study to maintain consistency of the data output mode. One of the reforecast products is 9-month hindcast for four cycles (0000, 0600, 1200, and 1800 UTC) of that day from every fifth day, starting January first each year for the period from 1982 to 2010 (Saha et al. 2014). The initial conditions of atmosphere and ocean come from the NCEP Climate Forecast System Reanalysis (CFSR; Saha et al. 2010). Some conventional data types and NRL WindSat ocean surface winds are assimilated by CFSv2.

b. *In situ observations*

In situ 10-m observations of land surface wind speed were obtained from HadISD, version 3.0 (Dunn et al. 2016; freely available at https://www.metoffice.gov.uk/hadobs/hadisd). The dataset includes 8139 stations held on the ISD from the National Oceanic and Atmospheric Administration (NOAA) National Centers for Environmental Information [NCEI, formerly the National Climatic Data Center (NCDC); Smith et al. 2011]. To remove spurious data while keeping true extremes, the climate variables of the stations were subjected to several automated, objective quality-control tests. For this study, we selected stations with consecutive observations using the following filtering principles: a monthly mean value of wind speed will be calculated only if there are more than 15 days of complete observations in the month; an annual mean value of wind speed will be calculated only when all 12 monthly mean values in the year are available (Zeng et al. 2018). After the filtering process, 1439 meteorological stations remained, all of them having 30 consecutive years of records over a period from 1989 to 2018. (The locations of the selected stations are shown in Fig. 2.)

For all months during 1989–2018, except for April 2015, there are more than 6000 stations with valid monthly mean wind speed (i.e., more than 15 days of observations); however, in April 2015, the number of valid stations decreased to 1010 (Fig. 1a). The process was repeated using the previous version of HadISD database (v2.0), which did not show a similar observation gap (Fig. 1b). Thus, the problem may be due to changes in quality-control tests for station selection and the merging processes new to the more recent version of HadISD (v3.0; Dunn et al. 2016). A fill-in process was implemented to maximize the number of stations with consecutive records. First, meteorological stations with valid monthly mean values for the other 11 months (except April) in 2015 were extracted from HadISDv3.0 and meteorological stations with valid monthly mean values for all 12 months in 2015 were extracted from HadISDv2.0. Then, stations identified in both versions were extracted. For the extracted stations, those that showed near perfect agreement in wind speed for the 11 months (except April) between the two versions (i.e., the ratio between the two versions should be above 99% confidence level) were identified. For these, the missing values for April 2015 in HadISDv3.0 were replaced with the values from HadISDv2.0.

An important consideration for verifying reanalysis data with observations is whether the observation dataset is independent data that have not been assimilated by reanalysis. The land surface winds observed in this study were not assimilated by all reanalysis data considered here. Therefore, the observed wind speed dataset from the in situ stations are independent of those reanalysis products.

c. *Methods of trend analyses and statistics*

Noting that wind speeds vary on multiple temporal scales, from subsecond (Schäfer et al. 2018) to multidecadal and centennial (Bett et al. 2017), this study focuses on variability on interannual time scales over the past three decades. During this period, Zeng et al. (2019) found that global terrestrial stilling reversed in 2010 and wind speeds over land rebounded to the level in the 1980s. Building on those findings, this study examines overall trends and piecewise trends of global/regional wind speeds around the turning points in the global reanalysis products. Because of the different spatial resolutions of the five reanalysis products, they are regridded to the same resolution using the nearest-neighbor interpolation method, that is, 721×1440. In essential, this regrid process does not really change their resolutions. We have verified that the results obtained by this method are almost the same as that by other interpolation

TABLE 2. Wind power density at 10 m, reference value of mean wind speed at 10 and 80 m, and the effect on wind power production for different classes of wind speed.

Class	Wind power density at 10 m ($W m^{-2}$)	Reference value of mean wind speed at 10 m ($m s^{-1}$)	Reference value of mean wind speed at 80 m ($m s^{-1}$)	Effect
1	<100	<4.4	<5.9	Poor
2	100–150	4.4–5.1	5.9–6.9	Poor
3	150–200	5.1–5.6	6.9–7.5	Good
4	200–250	5.6–6.0	7.5–8.1	Better
5	250–300	6.0–6.4	8.1–8.6	Best
6	300–400	6.4–7.0	8.6–9.4	Best
7	400–1000	>7.0	>9.4	Best

approaches, hence, it is appropriate to process the data in this method. Grid cells in closest proximity to station locations were then extracted for the regional and global comparisons. When multiple stations are located within a grid cell, the value of the same grid will be extracted multiple times to assign the same gridcell time series. Meanwhile, we note that this happens rarely, hence the impact on trend analysis is minimal.

We apply the Mann–Kendall (M-K) nonparametric test (Rehman 2013) and the Sen's slope estimation (Gocic and Trajkovic 2013) to quantify the wind speed trends for each period in each region. The M-K test is a nonparametric test, which means the data do not need to satisfy the normality assumption. Besides, the M-K test is also capable of testing a trend in nonlinear time series. Considering wind speed variations are not necessarily linear and may not follow normal distribution, the nonparametric approaches (the M-K test and the Sen's slope estimation) are chosen to estimate and test the trends. We apply a 95% confidence level in M-K test and use the upper and lower limits of the corresponding confidence interval of Sen slope value to present the uncertainty of the trends.

The turning point in annual mean wind speed series is identified automatically by the *segmented* package in the R software (https://cran.r-project.org/web/packages/segmented/segmented.pdf); meanwhile, this method can also automatically obtain the fitting equation of the wind speed series (Muggeo 2008). We obtain the best linear fitting that has the highest R squared (Muggeo 2003). This method requires a preliminary examination of initial values or number of turning points by visual inspection of time series and multiple sensitivity examinations of different initial values and number of turning points.

In terms of evaluating the overall performance of the reanalysis products, four statistical metrics are used to directly examine the differences in multiyear (1989–2018) average wind speed between reanalysis data and observations: standard deviation (STDE), root-mean-square error (RMSE), percent bias (PBIAS), and correlation coefficient squared R^2. We compare the differences at a global scale as well as in each region.

In wind power assessments, wind power density p is a key indicator used to evaluate the potential of wind energy. It is estimated using the following formula:

$$P_d = \frac{1}{2}\rho s f v^3, \tag{1}$$

where ρ is the air density, s is the area swept by the blades, f is an efficiency factor, and v is the wind speed (Lu et al. 2009). In this study, ρ, s, and f are assumed to be fixed values (constants) when calculating changes of wind energy production after the turning points. We do not consider the uncertainty caused by changes of other impact factors; rather, we only consider the changes of wind energy production caused by changes of wind speeds.

Since wind speed changes have a significant impact on wind energy production, we quantify wind energy changes utilizing wind speed change and compare the results of reanalysis products and observations. To study which level of wind speed has a significant change, annual mean wind speeds are classified into seven levels shown in Table 2 (Archer and Jacobson 2003, 2005). The changes in the frequency of wind speed at each level are then examined. To reflect the situation of typical height of commercial wind turbines (approximately 80 m), the 10-m winds are transformed to winds at 80 m using the exponential wind profile power-law relation:

$$\frac{U_2}{U_1} = \left(\frac{z_2}{z_1}\right)^{\alpha}, \tag{2}$$

where U_2 and U_1 represent wind speeds at heights z_2 (=80 m) and z_1 (=10 m), respectively, and α is a nondimensional wind shear exponent, which is typically set to 0.143 (i.e., 1/7) as used for land surface wind resource assessments under the assumption of neutral stability. When α is set as a constant value, it cannot be used to explain the stability of the atmosphere, the roughness of the land surface, and the zero-plane displacement. Where trees or structures impede land surface winds, using a constant exponent may introduce uncertainty. However, the difference between the two levels is usually not so great that large errors are introduced in the estimation. In addition, a constant α value (1/7) has been used widely in evaluating future wind energy production trends (Tian et al. 2019; Wang et al. 2016) and in developing the Wind Resource Map at the National Resource Energy Laboratory (Holt and Wang 2012).

3. Results

a. *Evaluation in the climatology of wind speeds between observations and reanalysis*

The climatology of wind speeds in those reanalysis products are evaluated by means of four statistical metrics calculated from the observations (STDE, RMSE, PBIAS, and R^2).

TABLE 3. The statistics in evaluating the climatology (multiyear average of 1989–2018) of wind speed between reanalysis products and observations in each region. The minimum error of each group is shown in boldface type for clarity.

Region	Reanalysis	STDE	RMSE	PBIAS (%)	R^2	Region	Reanalysis	STDE	RMSE	PBIAS (%)	R^2
Global	ERA5	**0.02**	**0.04**	**−4.54**	0.43	Europe	ERA5	**0.07**	**0.05**	**−5.61**	**0.79**
	ERA-Interim	0.03	**0.04**	9.09	0.58		ERA-Interim	0.09	0.06	10.21	0.78
	JRA-55	0.06	0.05	−54.22	**0.59**		JRA-55	0.13	0.09	−59.51	0.75
	CFSv2	0.06	0.07	−49.63	0.19		CFSv2	0.15	0.17	−69.34	−0.01
	MERRA-2	0.05	0.06	42.03	0.39		MERRA-2	0.14	0.09	41.61	0.76
North America	ERA5	0.04	0.13	−9.36	0.17	South America	ERA5	**0.04**	**0.06**	−8.00	0.66
	ERA-Interim	0.05	0.13	**0.58**	0.21		ERA-Interim	0.05	**0.06**	**2.70**	**0.70**
	JRA-55	0.05	**0.11**	−57.86	**0.62**		JRA-55	0.07	0.12	−44.01	−0.13
	CFSv2	**0.03**	0.14	−53.12	−0.20		CFSv2	0.06	**0.06**	−39.32	0.60
	MERRA-2	0.07	0.13	39.24	0.36		MERRA-2	0.05	0.07	36.14	0.46
Central Asia	ERA5	0.06	**0.11**	**16.13**	0.47	East Asia	ERA5	0.04	0.08	**8.69**	0.32
	ERA-Interim	0.06	**0.11**	27.40	**0.52**		ERA-Interim	0.05	**0.07**	25.10	**0.47**
	JRA-55	0.07	**0.11**	−53.34	0.43		JRA-55	0.06	0.08	−61.04	0.26
	CFSv2	**0.03**	**0.11**	−48.62	0.46		CFSv2	**0.03**	0.09	−45.24	−0.31
	MERRA-2	0.09	**0.11**	50.06	0.47		MERRA-2	0.08	0.09	50.53	0.30
Southeast Asia	ERA5	**0.03**	0.10	**−4.04**	−0.05	South Asia	ERA5	0.06	0.14	19.46	0.63
	ERA-Interim	0.04	0.10	14.62	−0.03		ERA-Interim	0.06	0.15	30.07	0.47
	JRA-55	0.06	0.10	−47.47	0.10		JRA-55	0.15	0.13	−38.82	0.66
	CFSv2	0.06	**0.08**	−16.57	**0.59**		CFSv2	**0.05**	0.18	**3.61**	−0.12
	MERRA-2	0.06	0.13	46.62	−0.29		MERRA-2	0.13	**0.11**	54.85	**0.76**
Africa	ERA5	**0.03**	0.04	−5.04	0.78	Australia	ERA5	0.05	**0.27**	−11.55	0.39
	ERA-Interim	0.05	**0.03**	**2.21**	**0.80**		ERA-Interim	0.06	0.28	**−5.06**	0.18
	JRA-55	0.12	0.13	−40.49	0.06		JRA-55	0.42	0.40	13.09	**0.40**
	CFSv2	0.09	0.07	−33.60	0.66		CFSv2	**0.04**	0.29	−47.17	−0.04
	MERRA-2	0.06	0.07	36.88	0.36		MERRA-2	0.08	0.29	26.53	−0.01
Mean	ERA5	**0.04**	**0.10**	**−0.39**	0.46						
	ERA-Interim	0.05	0.11	11.69	**0.47**						
	JRA-55	0.12	0.13	−44.37	0.37						
	CFSv2	0.06	0.13	−39.90	0.18						
	MERRA-2	0.08	0.11	42.45	0.36						

The results are summarized in Table 3, which describes the statistical comparison of each reanalysis and observations in different regions. The last group of this table shows the mean values of each metric for all regions.

The first notable feature in Table 3 is that ERA5 has a significant improvement in simulating land surface wind speed compared to its predecessor (ERA-Interim). Although their STDE and RMSE are very close in all regions, PBIAS of ERA5 is smaller than that of ERA-Interim in most regions, and hence the overall performance of ERA5 is better than ERA-Interim. In Europe, Southeast Asia, East Asia, and South Asia, as well as globally, the difference between ERA5 data and observed wind speed data is smaller than that of ERA-Interim. In terms of the climatology of wind speeds, the mean values of each error metric for all regions for ERA5 are smaller than that of other four reanalysis products (Table 3).

Analyzing the results by regions, JRA-55 and CFSv2 greatly underestimate the magnitude of observed wind speeds (negative PBIAS), and MERRA-2 largely overestimates the magnitude of observations (positive PBIAS). ERA-Interim slightly overestimates the observations in most regions. Except for central Asia, East Asia, and South Asia, ERA5 shows a slight underestimation in other regions. In terms of the mean errors for all regions, the climatology of wind speed in ERA5 is the closest to the observations. In addition, the correlation between reanalysis and observations has the most prominent performance in different regions: ERA5 in Europe (0.79), ERA-Interim in Africa (0.80), JRA-55 in North America (0.62), CFSv2 in Southeast Asia (0.59), and MERRA-2 in South Asia (0.76).

b. *Observed land surface wind speed trends for the period 1989 to 2018*

The majority of stations (774 of 1439 stations) show decreasing wind speed trends in North America (189 of 275; 69%), Europe (257 of 433; 59%), and East Asia (99 of 181; 55%) (Fig. 2). In these regions, annual mean wind speed significantly decreased at rates of -0.098 and $-0.103\,\mathrm{m\,s^{-1}\,decade^{-1}}$ in North America and South Asia, respectively ($p < 0.01$; Table 4). Wind speed does not significantly change in Europe, central Asia, and East Asia (Table 4). At a global scale, annual mean land surface wind speed declined by a trend of $-0.022\,\mathrm{m\,s^{-1}\,decade^{-1}}$ over the past 30 years (Table 4). This result is weaker than those of Vautard et al. (2010) and Wu et al. (2018), suggesting that the

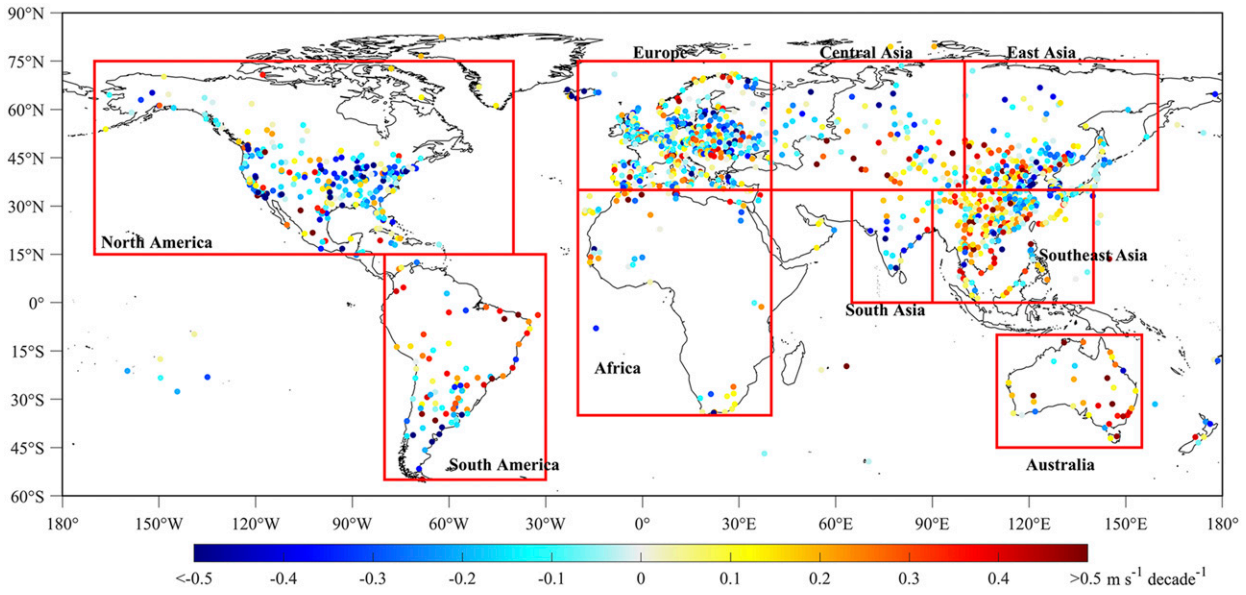

FIG. 2. Trend of annual mean land surface wind speed for each station for 1989–2018. The global continent is divided into nine regions: North America (15°–75°N, 170°–40°W); South America (55°S–15°N, 80°–30°W); Europe (35°–75°N, 20°W–40°E); Africa (35°S–35°N, 20°W–40°E); central Asia (35°–75°N, 40°–100°E); East Asia (35°–75°N, 100°–160°E); South Asia (0°–35°N, 65°–90°E); Southeast Asia (0°–35°N, 90°–140°E); Australia (45°–10°S, 110°–155°E).

wind speed trend in many regions has greatly changed in the last decade. This also confirms the study results by Zeng et al. (2019).

In contrast, wind speeds significantly increased in South America, Southeast Asia, Africa, and Australia (Table 4). The rising rates in these regions are 0.047, 0.074, 0.038, and 0.223 m s^{-1} decade^{-1}, respectively ($p < 0.01$; Table 4). In Australia, our analysis suggests that wind speed increased by 5% per decade relative to the 30-yr average wind speed. However, previous studies on Australian wind speed trends show mixed results. A study by McVicar et al. (2008) showed that 2-m wind speed has declined at a rate of -0.009 m s^{-1} yr^{-1} over Australia for the period 1975–2006. This result was confirmed by Troccoli et al. (2012) when analyzing 2-m wind speed trend ($-0.10 \pm 0.03\%$ yr^{-1}) for the same period. However, when using the 10-m wind, Troccoli et al. (2012) found that the trend was positive at a rate of $+0.90 \pm 0.03\%$ yr^{-1}, which is consistent with our findings. This difference may be partly attributed to observation height and the influence of surface roughness.

c. *Piecewise trends of observed land surface wind speed*

Wind speed at most stations around the world has different trends before and after 2010. As shown in Fig. 3a, the majority of stations (855 of 1439 stations; 59%) showed a downward trend during the period of 1989–2010, while most stations (939 of 1439 stations; 65%) showed an upward trend in the last decade (Fig. 3b) and the upward trends are steeper than the downward trends. Stations with increasing trends during 2010–18 account for 72% (618 of 855 stations) of the stations with decreasing trends during 1989–2010. More than 80% of

TABLE 4. Summary of the observed trends in regional 10-m wind speed for 1989–2018. A value with three stars indicates $p < 0.0$, n.s. indicates $p > 0.05$, a down arrow indicates negative trend, and an up arrow indicates positive trend. Trends and their 95% confidence levels are calculated with an M-K test.

Region	Mean during 1989–2018 (m s^{-1})	Trend during 1989–2018 (m s^{-1} decade^{-1}) and 95% confidence levels for trends	Significance levels	No. of stations
Global	3.287	−0.022 [−0.047, 0.007]	n.s.	1439
Europe	3.640	−0.032 [−0.077, 0.008]	n.s.	433
Central Asia	2.877	0.015 [−0.042, 0.086]	n.s.	84
East Asia	2.899	−0.021 [-0.057, 0.013]	n.s.	181
North America	3.382	−0.098 [−0.149, −0.048]	★★★(↓)	275
South America	3.456	0.047 [0.013, 0.078]	★★★(↑)	80
South Asia	2.411	−0.103 [−0.189, −0.034]	★★★(↓)	21
Southeast Asia	2.430	0.074 [0.040, 0.011]	★★★(↑)	231
Africa	3.683	0.038 [0.018, 0.057]	★★★(↑)	59
Australia	4.353	0.223 [0.138, 0.324]	★★★(↑)	34

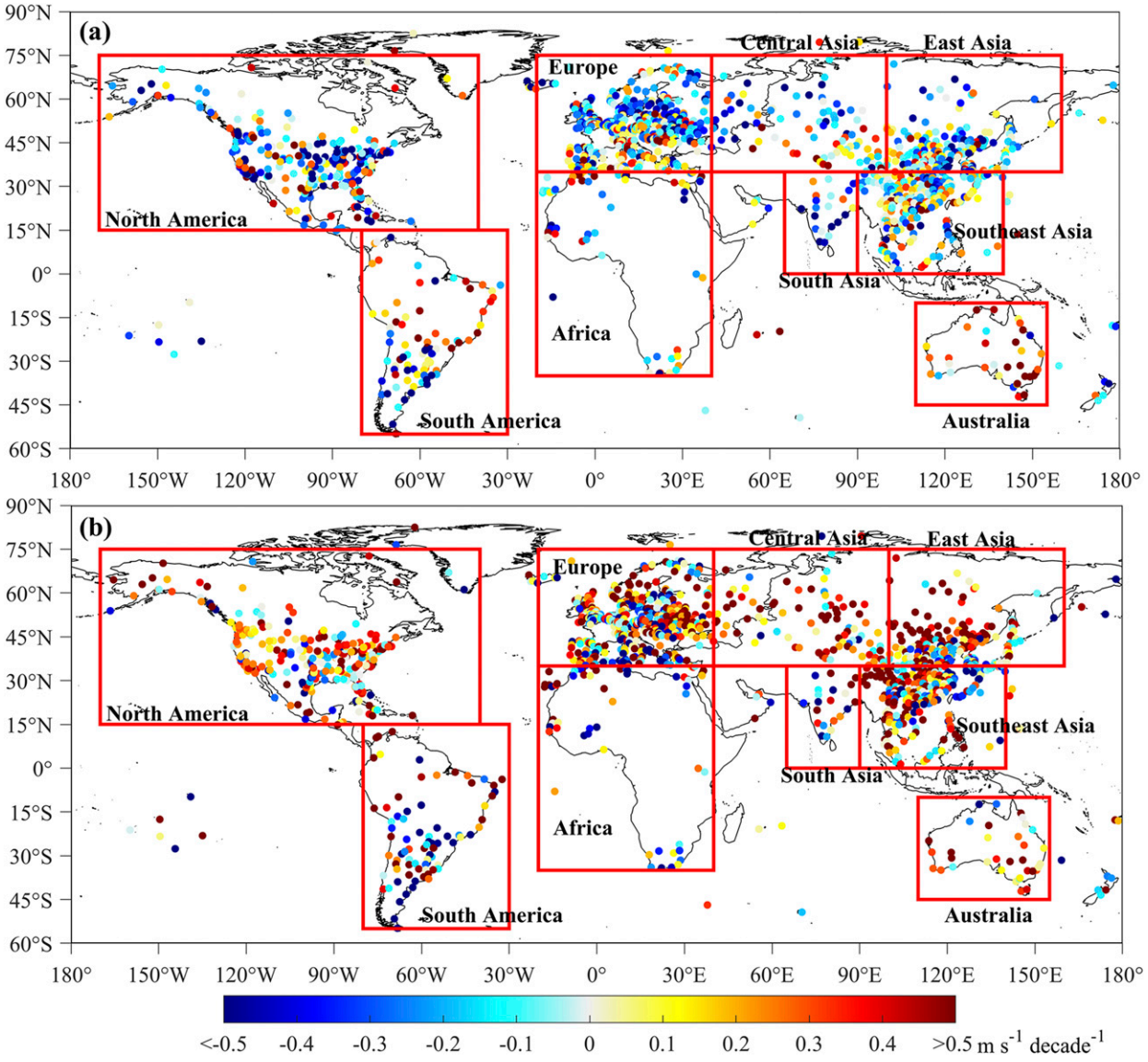

FIG. 3. Piecewise trends of observed land surface wind speed for (a) 1989–2010 and (b) 2010–18. Regions are as in Fig. 2.

stations with declining trends in central Asia and North America have reversed trends (Fig. 3). A rank of regions by the percentage of stations with declining trends during 1989–2010 in each region gives South Asia (17 of 21 stations; 81%), North America (188 of 275 stations; 68%), central Asia (54 of 84 stations; 64%), Europe (276 of 433 stations; 64%), East Asia (113 of 181 stations; 62%), Africa (31 of 59 stations; 53%), Southeast Asia (115 of 231 stations; 50%), South America (33 of 80 stations; 41%), and Australia (6 of 34 stations; 18%). Meanwhile, regions ranked by the percentage of stations with increasing trends during 2010–18 in each region are central Asia (54 of 84 stations; 81%), Australia (27 of 34 stations; 80%), North America (201 of 275 stations; 73%), East Asia (121 of 181 stations; 67%), Southeast Asia (145 of 231 stations; 63%), Europe (270 of 433 stations; 62%), Africa (32 of 59 stations; 54%), South Asia (11 of 21 stations; 52%), and South America (40 of 80 stations; 50%).

In the last decade, wind speed in most regions of the world has reversed in varying degrees since the global terrestrial stilling in 1960s (Fig. 4). Global mean wind speed significantly decreased at a rate of $-0.057\,\mathrm{m\,s^{-1}}$ (1.7%) $\mathrm{decade^{-1}}$ over the period of 1989–2010 ($p < 0.001$; Fig. 4a). However, wind speed rebounded in 2010 and then increased significantly at a rate of $0.181\,\mathrm{m\,s^{-1}}\,\mathrm{decade^{-1}}$ ($p < 0.001$; Fig. 4a), which is more than threefold the preceding decreasing rate, that is, an increase of up to almost 5% in the next 10 years. Globally, the trend and turning point of this study are consistent with that of Zeng et al. (2019), noting that our increasing trend is relatively weaker, partly because of a different station sample.

Here we confirm that the phenomenon of global terrestrial stilling occurred in the first two decades, especially in Europe,

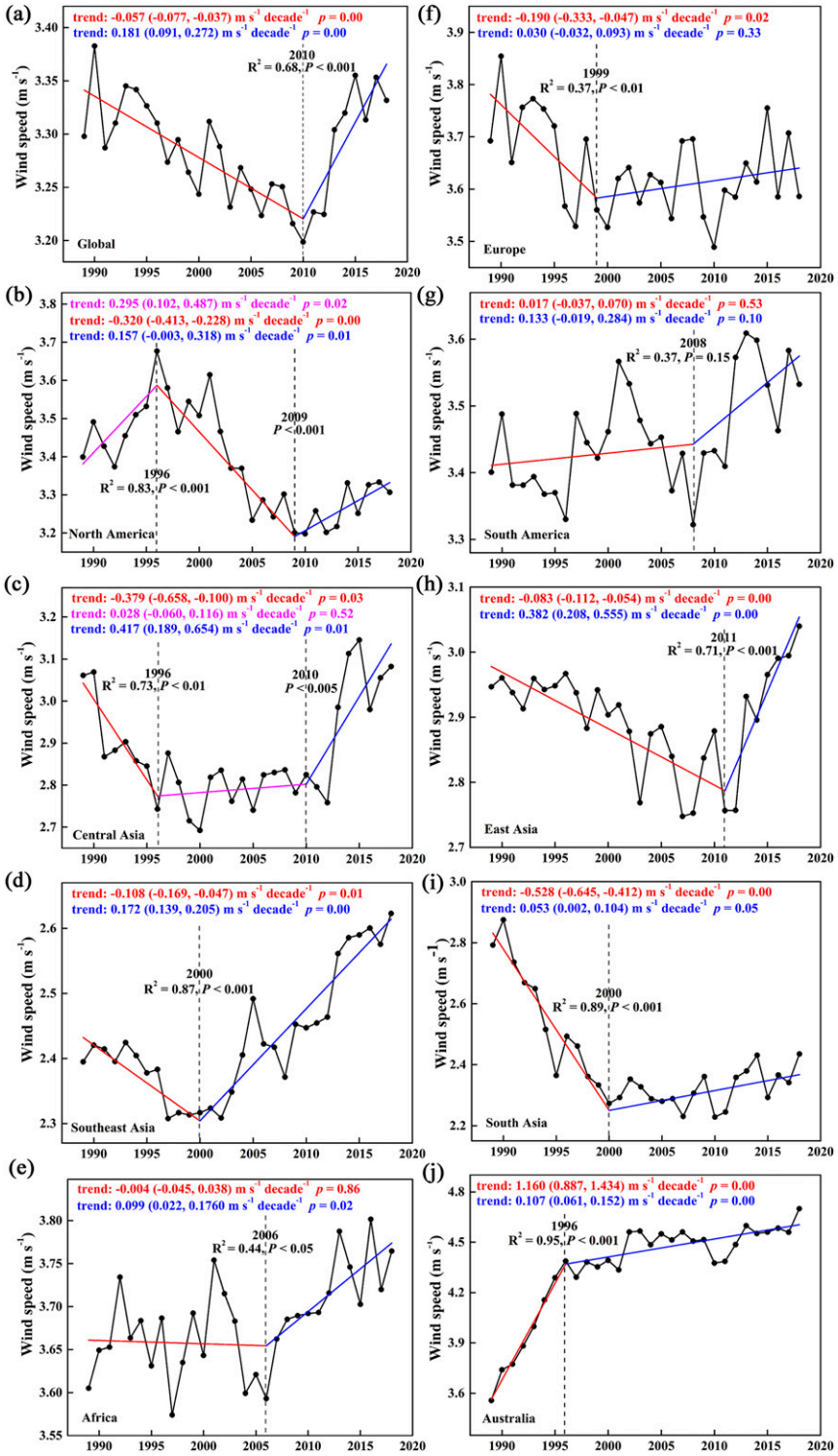

FIG. 4. Observed piecewise trends of the 10-m wind speed worldwide, showing time series of observed annual mean wind speed over the following regions: (a) global, (b) North America, (c) central Asia, (d) Southeast Asia, (e) Africa, (f) Europe, (g) South America, (h) East Asia, (i) South Asia, and (j) Australia. All piecewise linear trends were calculated by the *segmented* package in the R software. The numbers in parentheses are the 95% confidence intervals for piecewise trends from a *t* test. The intersection of the piecewise trends is the turning point.

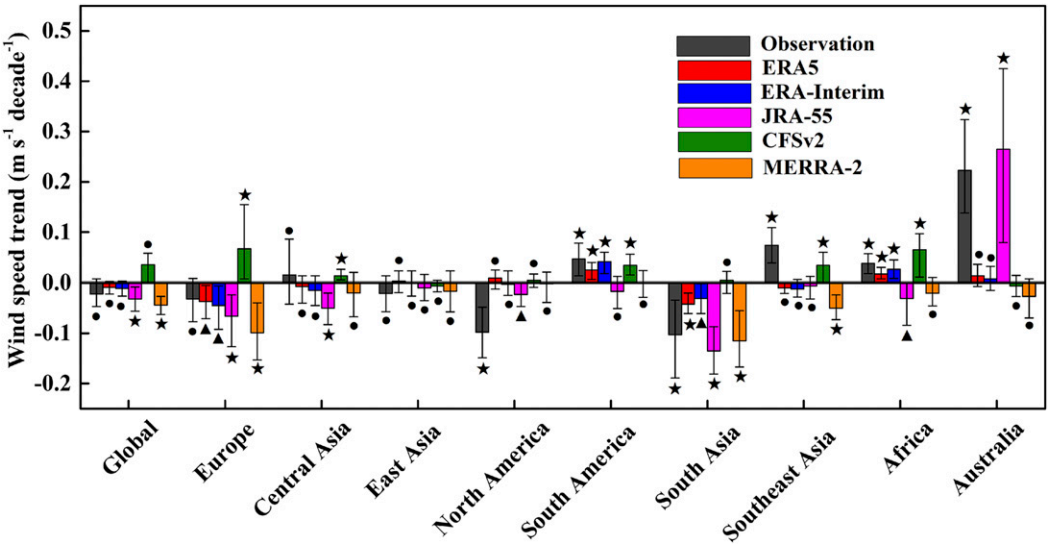

FIG. 5. Comparison on the overall trends during 1989–2018 in the observations against that in the five products. The gray, red, blue, pink, green, and orange bars represent observations, ERA5, ERA-Interim, JRA-55, CFSv2, and MERRA-2, respectively. The error bars show the upper and lower confidence limits of the Sen slope values with 95% confidence interval. Significance levels are expressed with stars, triangles, and circles, representing $p < 0.01$, $p < 0.05$, and $p > 0.05$, respectively.

North America, central Asia, East Asia, Southeast Asia, and South Asia, where the wind speed decreased significantly at rates of −0.190 (Fig. 4f), −0.320 (Fig. 4b), −0.379 (Fig. 4c), −0.083 (Fig. 4h), −0.108 (Fig. 4d), and $-0.528\,\mathrm{m\,s^{-1}\,decade^{-1}}$ (Fig. 4i), respectively. Significant turning points occurred in Europe (1999; $p < 0.01$; Fig. 4f), North America (2010; $p < 0.001$; Fig. 4b), central Asia (2010; $p < 0.01$; Fig. 4c), East Asia (2011; $p < 0.001$; Fig. 4h), Southeast Asia (2000; $p < 0.001$; Fig. 4d), South Asia (2000; $p < 0.001$; Fig. 4i), Africa (2006; $p < 0.05$; Fig. 4e), and Australia (1996; $p < 0.001$; Fig. 4j). The annual mean wind speed increased significantly at the rate of 0.030, 0.157, 0.417, 0.382, 0.172, 0.053, 0.099, and $0.107\,\mathrm{m\,s^{-1}\,decade^{-1}}$ in these regions after the turning points, or 0.8%, 4.9%, 14.8%, 13.9%, 7.4%, 2.3%, 2.4%, and 3.0% $\mathrm{decade^{-1}}$, respectively (Fig. 4). Although the turning point of wind speed trend in South America is not significant (2008; $p = 0.15$; Fig. 4g), after 2008, the wind speed has increased at a rate of $0.133\,\mathrm{m\,s^{-1}\,decade^{-1}}$ (4%). In North America, South America, central Asia, East Asia, and Africa, the turning points occurred in the last decade, but in Southeast Asia, South Asia, and Europe, the turning points occurred around 2000. Interestingly, wind speed persisted to increase over Australia during the period of 1989–2018. It increased rapidly at a high rate of $1.16\,\mathrm{m\,s^{-1}}$ (32.6%) $\mathrm{decade^{-1}}$ before 1996, followed by a slowdown (Fig. 4j). In addition, in central Asia and North America, there are two turning points. In central Asia, wind speed decreased significantly ($p < 0.05$) at a rate of $-0.379\,\mathrm{m\,s^{-1}}$ (12.4%) $\mathrm{decade^{-1}}$ before 1996, followed by a relatively stable period (1996–2010), and then a significant increase ($p < 0.05$) after 2010 (Fig. 4c). In North America, wind speed increased significantly ($p < 0.05$) before 1996, decreased significantly ($p < 0.01$) over the period of 1996–2009, and then increased significantly after 2009 at a rate of $0.157\,\mathrm{m\,s^{-1}\,decade^{-1}}$ ($p < 0.01$; Fig. 4b).

d. *Reanalysis land surface wind speed trends for the period 1989–2018*

There are noteworthy differences in the overall wind speed trends for the period 1989–2018 between the five reanalysis products and the observations, in terms of the direction (positive or negative) and magnitude of wind speed trends (Fig. 5). At a global scale, in contrary to the positive trend shown by CFSv2 and MERRA-2, all other products have negative trends like the observations. JRA-55 is most similar to the observed negative wind speed trend, whereas ERA-Interim and ERA5 underestimate the magnitude of the observed decreasing trend more than threefold, and MERRA-2 overestimates the magnitude by twice the amount of the observed trend. Regionally, when comparing ERA5 and ERA-Interim, ERA5 is more consistent with the observed trends in Europe, while ERA-Interim is more consistent with the observations in South America and Africa. In other regions, their performances in simulating observed trends are not very satisfactory. In Australia, there is a strong positive trend in the observations; JRA-55 captured this observed trend while all the other four products did not. The strong trend characteristics of JRA-55 are also reflected in South Asia, Europe, and central Asia. In terms of MERRA-2, its consistency with observations in South Asia and East Asia is better than other products. MERRA-2 shows a negative trend in all regions, including regions where the observed trend is positive, such as central Asia, Southeast Asia, Africa, and Australia. In central Asia and Southeast Asia, CFSv2 shows the same positive trend as found in the observations, noting that the observed rates are underestimated.

To reveal the interannual variability of land surface wind speed for the period of 1989 to 2018, the observed time series of annual mean wind speed are compared with that from five reanalysis products (Fig. 6). At a global scale, no products show significant agreement with observations (Fig. 6a). The interannual variabilities in ERA5 and ERA-Interim are close to observations before 2006. However, they both show poor performances after 2006. JRA-55 shows robust interannual variability as compared with the other reanalysis in most regions, especially in Australia where JRA-55 has the strongest interannual fluctuation of wind speed (Fig. 6j). A further examination of the regional mean trend in Figs. 6b–j finds that ERA5 and ERA-Interim show greater agreement with the observed variabilities than other products in Europe (Fig. 6f), and ERA-Interim agrees well with the observations in Africa (Fig. 6e). No reanalysis data closely resemble the observations in other regions, and none of the reanalysis data perform well in reproducing the turning points in all regions.

e. *Piecewise trends of reanalysis land surface wind speed*

Figure 7 shows the comparisons of the reanalysis products against observations with regard to piecewise trends of annual mean wind speed at the global scale and the nine regions. The different periods are based on the turning points calculated from the observations as shown in Fig. 4. None of these reanalysis products captures the piecewise trends for the whole different regions. At the global scale, all five reanalysis products and the observations show a negative trend of wind speed over the period of 1989–2010. Among them, while both JRA-55 and MERRA-2 reproduce the observed significant and negative trends (both with $p < 0.01$), JRA-55 is closer to the observations ($-0.059\,\mathrm{m\,s^{-1}}$ decade^{-1} in JRA-55 vs $-0.062\,\mathrm{m\,s^{-1}}$ decade^{-1} in the observations). However, as for the recent reversal, no product captured the significant increasing trend in the past decade (Fig. 7a).

At a regional scale, the trends in the reanalysis products are less frequently significant in comparison with those in observed data. Relative to observed trends, reanalysis trends are sometimes greater or weaker in magnitude, and sometimes of opposite sign (Figs. 7b–j). This uncertainty has been reported by many previous studies (Pryor et al. 2009; Pryor and Barthelmie 2010). In Southeast Asia, while ERA5 ($p < 0.05$), ERA-Interim ($p < 0.05$), and MERRA-2 ($p < 0.01$) have captured the phenomenon of terrestrial stilling during 1989–2000, only the magnitude of wind speed trend in MERRA-2 is similar to the observations. After the turning point, only CFSv2 captures the observed significant and positive trend ($p < 0.01$), while other reanalysis products greatly underestimate the observed wind speed trend after 2000. In South America, it also performs best after the turning point. Therefore, CFSv2 is the best choice for wind energy users who want to use reanalysis data to evaluate wind energy output in Southeast Asia and South America in the recent decade. Not only in Southeast Asia, but also in South Asia, MERRA-2 shows a significant downward trend consistent with observations before the turning point ($p < 0.01$). After the turning point, however, none of the reanalysis products shows the same positive and significant wind speed trend as the observations ($p < 0.05$). Contrary to the situation in South Asia, MERRA-2 in East Asia is closest to the observed trend after the turning point among all reanalysis products (Fig. 7h). CFSv2 captures the positive trends in Africa (Fig. 7e) and Europe (Fig. 7f), but it largely overestimates the magnitude of the observed increasing trend. In Europe (Fig. 7f), JRA-55 performs best before the turning point; in Africa (Fig. 7e), the wind speed trend of ERA-Interim is the most similar to observations after the turning point. There are two turning points in central Asia (Fig. 7c) and North America (Fig. 7b). In terms of the recent reversal of wind speed trends, only ERA-Interim and JRA-55 have very weak positive trend after the turning point in North America (Fig. 7b); EAR-Interim shows the most consistent trend with observations. The observed wind speed in Australia increased significantly for both 1989–96 and 1996–2018 ($p < 0.01$; Fig. 7j), while these reanalysis products show very weak positive trend in both periods, except for JRA-55, which overestimates the observed increasing trend after the turning point.

4. Discussion

a. *Inconsistent wind speed trends between reanalysis and observations*

There are large inconsistencies in the land surface wind speed trends between reanalysis products and observations, regardless of whether overall trends or piecewise trends are considered. Given uncertainties of different reanalysis products, in a global context no product shows overall better performance. Therefore, for the wind energy industry, it is important to determine which product is more suitable for predicting the wind speed trend in different regions.

The overall observed trends have been best captured by JRA-55 at a global scale, while regionally observed trends are more consistent with ERA5 in Europe, with ERA-Interim in South America and Africa, with JRA-55 in Australia, with CFSv2 in central Asia and Southeast Asia, and MERRA-2 in South Asia and East Asia. In terms of the interannual variability of land surface wind speed, ERA5 or ERA-Interim shows greater agreement with the observed variabilities than other products in Europe. Meanwhile, there is the lowest difference in the climatology of wind speed between ERA5 and observations in Europe. The mean values of the error metrics also describe the same result, that is, the wind speeds of ERA5 are the closest to the observations as for the climatology.

The piecewise trends show wind speed trends calculated by reanalysis data have been significantly underestimated compared to the observed piecewise trends in most regions. This is consistent with the results obtained by Coburn (2019). JRA-55 can capture the phenomenon of global terrestrial stilling well, especially the stilling in Europe, North America, and Africa. Meanwhile, MERRA-2 not only captures the stilling in Southeast Asia and South Asia but also has a good performance in reproducing the recent increasing wind speed in the observations in East Asia. As for ERA-Interim, it performs best in central Asia after the turning points. CFSv2 may by a good choice if wind users want to predict the wind speed trends in South America and Southeast Asia in the

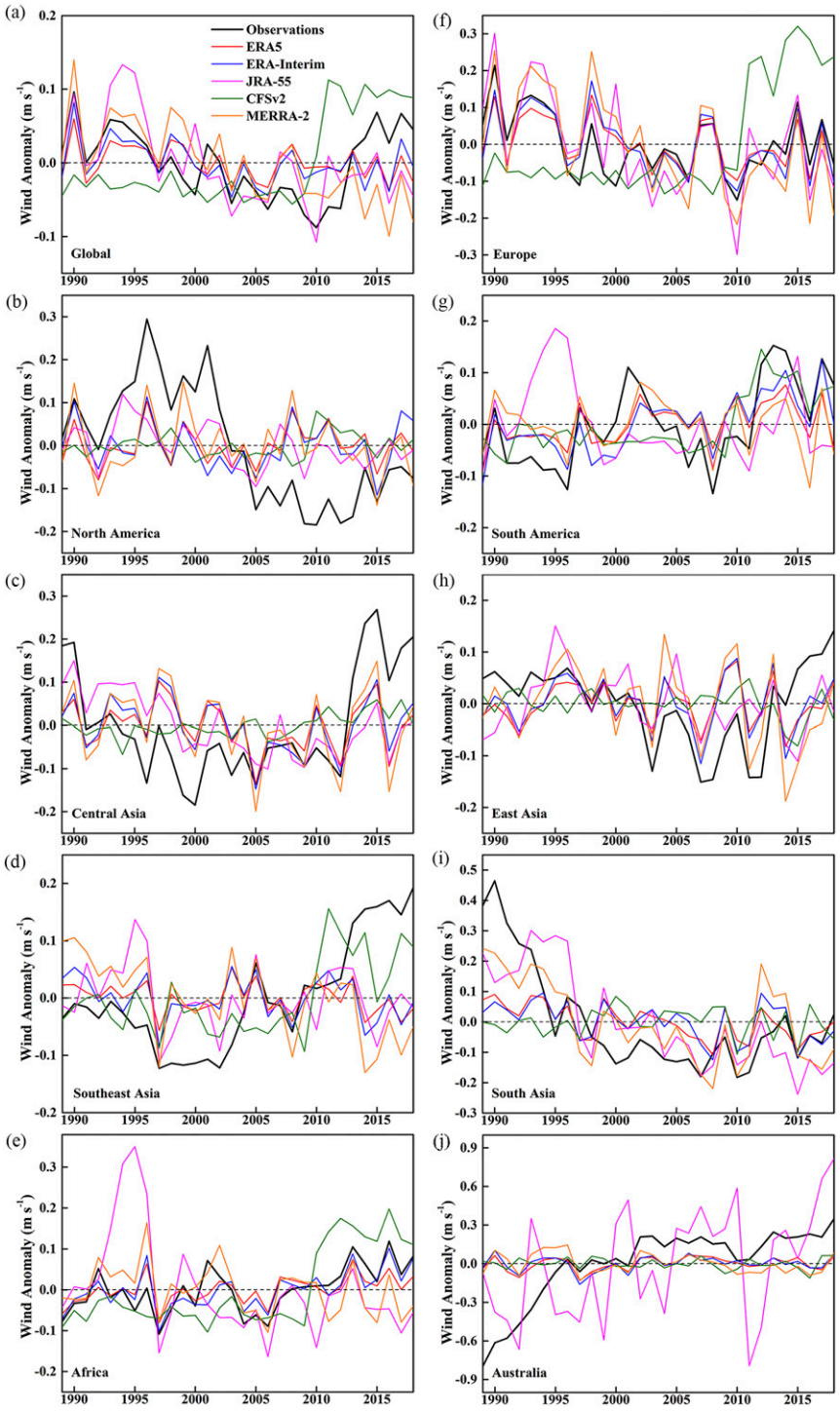

FIG. 6. Anomalies of wind speed in the five global reanalysis products and the observations in the following regions: (a) global, (b) North America, (c) central Asia, (d) Southeast Asia, (e) Africa, (f) Europe, (g) South America, (h) East Asia, (i) South Asia, and (j) Australia. Black, red, blue, purple, green, and orange solid line represent the observations, ERA5, ERA-Interim, JRA-55, CFSv2, and MERRA-2, respectively.

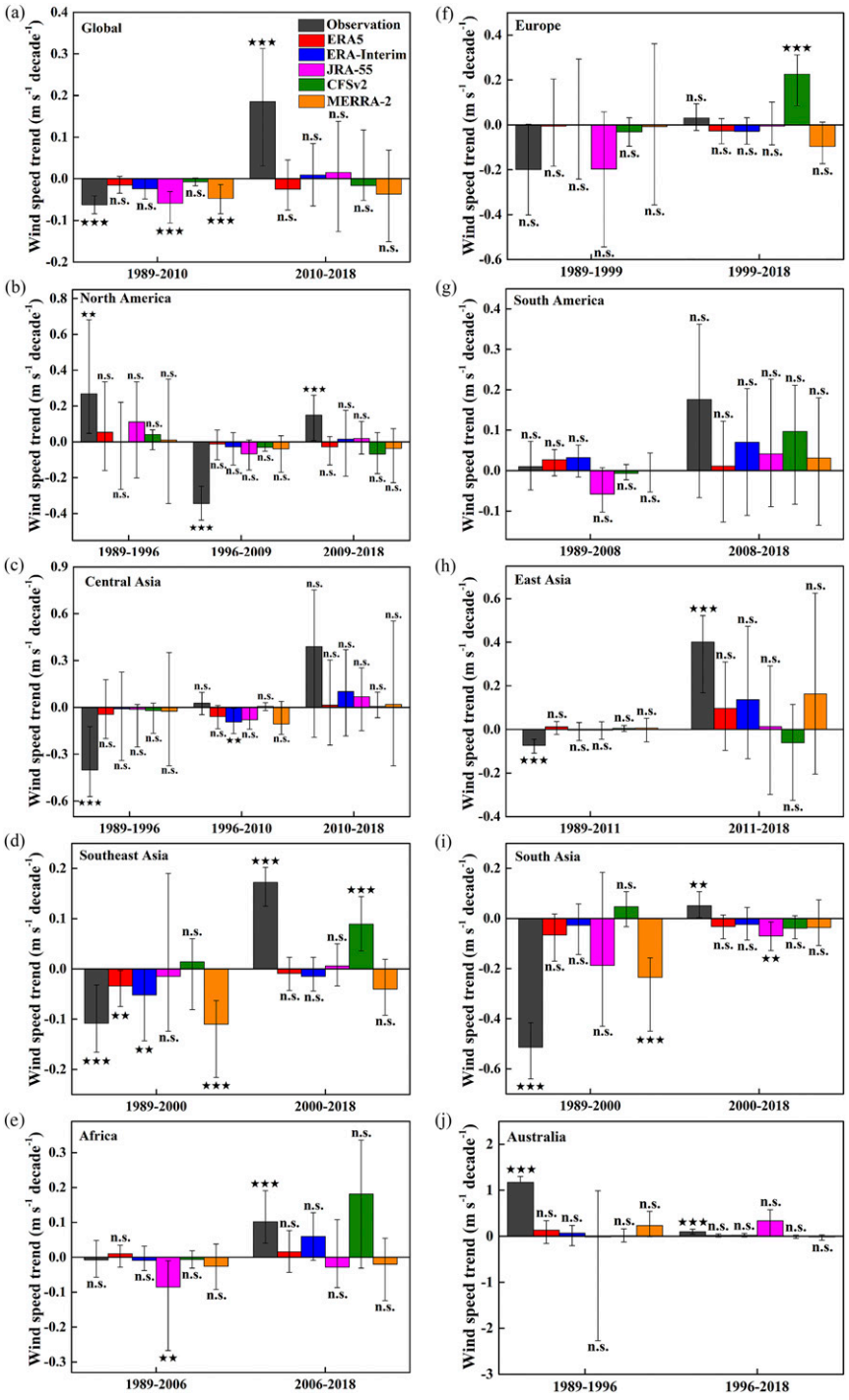

FIG. 7. Comparisons of the piecewise trends of the five reanalysis products with the observations in the following regions: (a) global, (b) North America, (c) central Asia, (d) Southeast Asia, (e) Africa, (f) Europe, (g) South America, (h) East Asia, (i) South Asia, and (j) Australia. The gray, red, blue, pink, green, and orange bars represent observations, ERA5, ERA-Interim, JRA-55, CFSv2, and MERRA-2, respectively. The different periods are divided by the segmentation points detected in Fig. 3. The trends and their 95% confidence intervals of Sen slope are calculated in each segment period using an M-K test. Significance levels are expressed with three stars, two stars, and n.s., representing $p < 0.01$, $p < 0.05$, and $p > 0.05$, respectively.

recent decade. However, as CFSv2 and JRA-55 largely overestimate the magnitude of observed wind speed trends in Europe and Australia, respectively, there are currently no suitable products to estimate recent wind speed trend in these two regions.

b. *Potential causes of inconsistency*

The inconsistencies between reanalysis products and observations can be expected to some extent because they have similar physical assumptions and similar observed data assimilation. Their inconsistencies may be due to the following reasons:

1) In terms of reanalysis 10-m wind speed trends, the deviation among products may be attributed to different assimilation data types (Carvalho 2019; Rose and Apt 2016). All reanalysis products considered here ingest the same types of conventional inputs including ships, drifting buoys, aircraft records, radiosonde profiles, and satellite measurements (QuikSCAT, *ERS-1*, and *ERS-2*, SSM/I). In addition to these inputs, CFSv2 and MERRA-2 also assimilate the data from NRL WindSat, JRA-55 and MERRA-2 also assimilate the ASCAT ocean surface winds, ERA5 assimilates various newly reprocessed datasets and recent instruments that could not be ingested in ERA-Interim, and ocean surface winds from moored buoys are also assimilated by MERRA-2. It is worth noting that no reanalysis products ingest land surface winds from in situ observations very well. This is due to inadequate simulation of inhomogeneous terrain and atmospheric boundary layer conditions in the process of data assimilation.
2) Wind speeds are parameterized in the boundary layer scheme according to the land surface characteristics and stability in the process of extrapolation from the lowest model level to 10 m. Therefore, different methods of vertical extrapolation also lead to inconsistent trends of reanalysis wind speeds. ERA5 and ERA-Interim use the modified Monin–Obukhov scheme by adjusting aerodynamic roughness length according to orographic drag. CFSv2 interpolates the wind speed at the lowest model level to 10 m according to the Monin–Obukhov similarity functions from the NCEP Noah land surface model with fixed aerodynamic roughness length for a given cover type, static over time. The Helfand and Schubert scheme based on Monin–Obukhov similarity theory is used to interpolate the 10-m winds in MERRA-2. Under the assumption of neutral stability, JRA-55 extrapolates the wind speed of the lowest level model to 10 m by using a univariate two-dimensional optimal interpolation method. According to Torralba et al. (2017), because the lowest level is placed too high in the forest covered area, the extrapolated wind speeds may be significantly reduced. These different data processing methods may affect the wind speed trends.
3) The inconsistent wind speed trends between the reanalysis products and the observed wind speeds may also be caused by the scale differences. Each grid value in the gridded reanalysis product represents the mean wind speed over area. As the area increases there will be a tendency for the mean value to decrease. The areal estimates will show considerably less variability compared to the observed station value. Especially in the regions with heterogeneous terrain and wind speed with high spatiotemporal variability, the gridded spatial variability of wind speed will be smaller (smoother over space). Our results show that the magnitude of wind speed in ERA5 is closest to the observations, which may be due to the relatively high spatial resolution of ERA5 compared with other reanalysis products.
4) Because wind speed is based on model estimation, differences between reanalysis products may also be attributed to the quality of the climate model. Vautard et al. (2010) found that most reanalysis products (e.g., NCEP–NCAR and ERA-Interim) did not capture the observed trend in surface wind speed over land (i.e., the global terrestrial stilling). By presuming that the models are perfect in simulating climate dynamics but neglecting changes in surface roughness, they attributed the global terrestrial stilling to increasing surface roughness caused by the increased vegetation activities in the past several decades. However, the recent study by Zeng et al. (2019) mainly attributed previous stilling and recent reversal of terrestrial wind speeds to large-scale ocean–atmosphere oscillations, mainly related to the tropical Northern Atlantic index (TNA), the North Atlantic Oscillation (NAO), and the Pacific decadal oscillation (PDO). The previous assumption should not be valid, and those climate models used to generate reanalysis products may have caveats in reproducing the changes in ocean–atmosphere oscillations. It should be noted that the reasons for the changes in wind speeds are still controversial, as the measured wind speed captures changes mainly to surface roughness and atmospheric stability (Barthelmie 1999), not all factors have been identified and quantified, which makes it difficult to determine the underlying mechanisms for wind speed trends. Therefore, the physical mechanism of wind speed changes needs to be further studied and then evaluated in those models in depth.
5) The wind speed trend of reanalysis products may be false due to the continuous development of wind speed measurement technology. It is difficult to distinguish the satellite derived real wind speed changes for the evolution of satellite observing system. For example, the introduction of ATOVS into the CFSR data assimilation system around 1999 directly led to a significant reduction in wind speed in the late 1990s (Xue et al. 2011). In addition, the introduction of *ERS-1* surface winds in 1991, the failure of QuikSCAT in 2009 and the discontinuation of *ERS-2* in 2011 all affected the global wind speed trend observed by satellite (Wen et al. 2019).

Although we have evaluated the wind speed trends in this study, the results are preliminary as we have yet to assess sporadic and systematic influence of sources of uncertainties, such as those listed above and influences, such as regional and global changes in aerodynamic roughness. However, given the uncertainty of any product in evaluating the long-term trend of wind speed in the twentieth century, wind energy users may use

TABLE 5. Changes in wind energy production after the turning points. Numbers that are closest to observations (Obs) are indicated with boldface type.

Region	Turning point	Obs	ERA5	ERA-I	JRA-55	CFSv2	MERRA-2
Global	2010	13%	−2%	0.6%	**14%**	15%	−2%
Europe	1999	2%	**−10%**	−11%	−11%	144%	−13%
North America	2009	10%	−3%	5%	16%	**9%**	−4%
South America	2008	20%	0.1%	6%	7%	**16%**	2%
Central Asia	2010	30%	−2%	1%	**9%**	−2%	−1%
East Asia	2011	34%	**11%**	10%	−6%	−14%	9%
Southeast Asia	2000	45%	1%	1%	−2%	**17%**	−2%
South Asia	2000	23%	**−2%**	−4%	−21%	−15%	−5%
Africa	2005	12%	3%	**8%**	−1%	25%	3%
Australia	1996	23%	2%	**5%**	100%	2%	−3%

this comparison information to decide which product to select according to their study regions.

c. *Assessments of wind resource from five products and observations*

As global reanalysis products are widely used for wind power assessments, we compared and analyzed the wind energy production changes calculated by reanalysis products and observations after the turning point in each region (Table 5). Based on the global average wind speeds rising from 3.19 m s^{-1} in 2010 to 3.33 m s^{-1} in 2018, potential wind energy production increased by 13%. Among these reanalysis products, the growth rate of JRA-55 is closest to the observations at a global scale, which is consistent with the best product selected for judging wind speed trend. Regionally, recent increasing wind speed trends have led to rapid growth in potential wind energy production after the turning points in Asia, including the increasing by 45% in Southeast Asia, 34% in East Asia, 30% in central Asia, and 23% in South Asia. In addition, potential wind energy production in South and North America, Africa, Australia, and Europe has increased by 20%, 10%, 12%, 23%, and 2%, respectively. Despite relatively slow growth of wind energy in Europe, the trends of potential wind energy production in all regions is positive in recent decades.

These results suggest that wind energy could play an important role in the development of renewable energy and highlight regions of particular interest for future development, such as Asia. In these regions, wind power trend of observations is consistent with CFSv2 in North and South America and Southeast Asia, with JRA-55 in central Asia, with ERA-Interim in Africa and Australia, and with ERA5 in Europe, East Asia, and South Asia. As reanalysis products seriously overestimate or underestimate observed wind energy changes in Europe and Australia, wind energy users need to be cautious when using reanalysis products to predict wind power production. In Europe, Southeast Asia, and at the global scale, the best product for estimating the wind energy trend is consistent with the best product for reproducing increasing wind speed trend after the turning point, noting inconsistencies in other regions. This is because the wind power change calculated by this study is for the year 2018 and the year when the turning point occurred. Although there is an upward trend of wind speed in time series in each region, the best products are also inconsistent due to the large fluctuation of wind speed. Therefore, when predicting the wind power change of each region, the product consistent with the observed wind speed trend is preferred. These assessments can provide a reference for wind energy companies when selecting the reanalysis products to predict future wind energy production.

Considering that most global wind turbines were installed in the past decade, we particularly evaluated the trends in wind speed after the turning points separating different speed levels for wind resources for each region (Table 6). We first applied the wind profile law (Wang et al. 2016) to the station-observed wind speeds at 10 m to the wind speeds at 80 m, a typical height of wind turbines. Wind speed less than 3 m s^{-1} cannot be used by turbines since the cut-in wind speed of turbines is 3 m s^{-1}. When wind speed is less than 6.9 m s^{-1}, an 80-m-high wind power turbine has poor power output. Table 5 shows that, at a global scale, the trends of wind speed distribution at all levels are positive. According to formula (1), the global potential wind energy production is an uptrend in the past decade. In the regional scale, wind speeds at low speed level are increasing significantly in each region, and in Europe, North America, central Asia, and Africa, wind speeds at high speed levels are positive, which can be used to infer that the strengthen wind has boosted the wind power generation as wind power generation largely depends on high wind speeds. Especially in Africa, the increasing trend is stronger than other regions in each level. However, because wind speed is low in South Asia, there are no changes in the distribution of wind speed at high speed level. This may indicate a slower increase in wind energy production in South Asia and it is not suitable to install turbines with larger capacities. This information indicates that turbines need to be optimized to improve production efficiency in order to adapt to wind speed changes in different regions.

5. Conclusions

In this study, we first evaluate the climatology of wind speeds between observations and all reanalysis products and find that ERA5 is the closest to the observation with regard to the climatology. ERA5 has a great improvement when compared with ERA-Interim. JRA-55 and CFSv2 underestimate the magnitude of observed wind speeds, while MERRA-2 and ERA-Interim overestimate the magnitude of observations.

TABLE 6. Trends in wind speed at different wind speed levels ($m\,s^{-1}$) for the period after the turning points. Values with two stars indicate $p < 0.01$, and one star indicates $p < 0.05$. Trends and their 95% confidence levels are calculated with an M-K test.

	>3	>5.9	>6.9	>7.5	>8.1	>8.6	>9.4
Global (2010–18)	0.902**	0.278*	0.019	0.036	0.040	0.001	0.023
Europe (1999–2018)	0.260**	0.023	0.021	−0.013	0.013	0.026	−0.017
North America (2009–18)	0.633**	0.282*	0.033	0.134	0.033	—	—
South America (2008–18)	0.534**	0.648*	−0.034	−0.148	−0.114	−0.114	0.114
Central Asia (2010–18)	2.242*	0.258	0.139	0.060	0.079	−0.040	—
East Asia (2011–18)	1.842*	0.829**	0.105	0.046	−0.079	—	—
Southeast Asia (2000–18)	0.444**	−0.015	−0.011	0.005	−0.008	−0.028	−0.008
South Asia (2000–18)	0.861**	−0.100	—	—	—	—	—
Africa (2006–18)	0.289*	0.326**	0.438**	0.270*	0.158	0.093	0.047
Australia (1996–2018)	0.061	0.372**	−0.145*	−0.041	−0.012	−0.061	—

The focus of this study is to investigate the trend of global land surface wind speed in five widely used global reanalysis products relative to in situ observations from 1439 meteorological stations with continuous records for the period 1989–2018. The observations show that the overall wind speed trend during 1989–2018 is negative globally but positive for South America, Southeast Asia, central Asia, Africa, and Australia. The piecewise trend analysis further shows that wind speed in many regions where stilling occurred has reversed and has been increasing fast in the past decade. The regions where wind speed is significantly increasing include North America ($p < 0.01$), central Asia ($p < 0.01$), East Asia ($p < 0.001$), Southeast Asia ($p < 0.001$), Africa ($p < 0.05$), South Asia ($p < 0.05$), and Australia ($p < 0.001$).

We analyzed the consistency of land surface wind speed trends shown in reanalysis products and observations. Results show that the products are highly uncertain in reproducing the observed decadal variations of wind speed at the global and regional scale. The trend of wind speed between reanalysis products and the observations lacks consistency, possibly due to the scale differences, the quality of the atmospheric model, the data assimilation methods, the availability of observations, and the continuous development of wind speed measurement technology.

No reanalysis product shows outstanding performance in capturing turning points in all the regions. In most regions, except for the strong trend characteristics in JRA-55, all other products significantly underestimate the observed wind speed variations. In terms of land surface wind speed stilling before the turning point, it is reasonably captured by JRA-55 on a global scale, Europe, and North America; by MERRA-2 in South Asia and Southeast Asia; by ERA5 in central Asia; and by ERA-Interim in Africa. Meanwhile, in terms of the recent increasing wind speed trend, CFSv2 can reasonably reproduce it in South America and Southeast Asia, while JRA-55 can reproduce it for North America and the global scale, ERA-Interim can reproduce it for central Asia and Africa, and MERRA-2 can reproduce it for East Asia. In addition, in Europe and Australia, there is no suitable reanalysis product to reproduce the recent upward trend closing to the observations. These findings are very helpful for wind energy users to select appropriate reanalysis products when evaluating wind speed trends and predicting wind energy production in different regions. If, as suggested by Zeng et al. (2019), the current growth trend continues for at least the next decade, the global wind energy production will increase dramatically.

In this study, due to limitations in the observational data sample in HadISDv3.0, the processing of observations may have a slight impact on the analysis of wind speed trend. High-quality and long-term in situ observations are necessary for examining long-term wind speed trend. They are not only used to verify reanalysis products, but also for other applications, such as modeling. In the regions without observations covered, reanalysis products are still the first choice for researchers and users.

This study provides guidance in selecting a reanalysis dataset for long-term wind energy assessments, noting that large discrepancies between data sources indicate that users need to be cautious when selecting any single dataset for an assessment. In a future analysis, we can quantify the uncertainty in the assessment and make the results more confident. Only in this way can wind companies better predict the potential changes of wind energy production in the future and get greater economic benefits.

Acknowledgments. This study was supported by the National Natural Science Foundation of China (42071022), the start-up fund provided by Southern University of Science and Technology (29/Y01296122), and the Highlight Project on Water Security and Global Change of the Southern University of Science and Technology (SUSTech; Grant G02296302).

Data availability statement. All data in this study are freely available on the website in Table 1. The observed wind data are two versions of HadISD, including v.2.0.2.2017f and v3.0.0.2018f. Five reanalysis products were used, including ERA5, ERA-Interim, MERRA-2, JRA-55, and CFSv2. More information is given in section 2.

REFERENCES

Archer, C. L., and M. Z. Jacobson, 2003: Spatial and temporal distributions of U.S. winds and wind power at 80 m derived from measurements. *J. Geophys. Res.*, **108**, 4289, https://doi.org/10.1029/2002JD002076.

——, and ——, 2005: Evaluation of global wind power. *J. Geophys. Res.*, **110**, D12110, https://doi.org/10.1029/2004JD005462.

Barthelmie, R. J., 1999: The effects of atmospheric stability on coastal wind climates. *Meteor. Appl.*, **6**, 39–47, https://doi.org/10.1017/S1350482799000961.

Bett, P. E., H. E. Thornton, and R. T. Clark, 2017: Using the Twentieth Century Reanalysis to assess climate variability for the European wind industry. *Theor. Appl. Climatol.*, **127**, 61–80, https://doi.org/10.1007/s00704-015-1591-y.

Carvalho, D., 2019: An assessment of NASA's GMAO MERRA-2 reanalysis surface winds. *J. Climate*, **32**, 8261–8281, https://doi.org/10.1175/JCLI-D-19-0199.1.

——, A. Rocha, M. Gómez-Gesteira, and C. S. Santos, 2014: Offshore wind energy resource simulation forced by different reanalyses: Comparison with observed data in the Iberian Peninsula. *Appl. Energy*, **134**, 57–64, https://doi.org/10.1016/j.apenergy.2014.08.018.

Coburn, J. J., 2019: Assessing wind data from reanalyses for the upper Midwest. *J. Appl. Meteor. Climatol.*, **58**, 429–446, https://doi.org/10.1175/JAMC-D-18-0164.1.

Dee, D. P., and Coauthors, 2011: The ERA-Interim reanalysis: Configuration and performance of the data assimilation system. *Quart. J. Roy. Meteor. Soc.*, **137**, 553–597, https://doi.org/10.1002/qj.828.

Dunn, R. J., K. M. Willett, D. E. Parker, and L. Mitchell, 2016: Expanding HadISD: Quality-controlled, sub-daily station data from 1931. *Geosci. Instrum. Methods Data Syst.*, **5**, 473–491, https://doi.org/10.5194/gi-5-473-2016.

Gelaro, R., and Coauthors, 2017: The Modern-Era Retrospective Analysis for Research and Applications, version 2 (MERRA-2). *J. Climate*, **30**, 5419–5454, https://doi.org/10.1175/JCLI-D-16-0758.1.

Gocic, M., and S. Trajkovic, 2013: Analysis of changes in meteorological variables using Mann–Kendall and Sen's slope estimator statistical tests in Serbia. *Global Planet. Change*, **100**, 172–182, https://doi.org/10.1016/j.gloplacha.2012.10.014.

Hersbach, H., and D. Dee, 2016: ERA5 reanalysis is in production. *ECMWF Newsletter*, No. 147, ECMWF, Reading, United Kingdom, 7, http://www.ecmwf.int/sites/default/files/elibrary/2016/16299-newsletter-no147-spring-2016.pdf.

Hobbins, M., A. Wood, D. Streubel, and K. Werner, 2012: What drives the variability of evaporative demand across the conterminous United States? *J. Hydrometeor.*, **13**, 1195–1214, https://doi.org/10.1175/JHM-D-11-0101.1.

Holt, E., and J. Wang, 2012: Trends in wind speed at wind turbine height of 80 m over the contiguous United States using the North American Regional Reanalysis (NARR). *J. Appl. Meteor. Climatol.*, **51**, 2188–2202, https://doi.org/10.1175/JAMC-D-11-0205.1.

Keyhani, A., M. Ghasemi-Varnamkhasti, M. Khanali, and R. Abbaszadeh, 2010: An assessment of wind energy potential as a power generation source in the capital of Iran, Tehran. *Energy*, **35**, 188–201, https://doi.org/10.1016/j.energy.2009.09.009.

Kim, J., and K. Paik, 2015: Recent recovery of surface wind speed after decadal decrease: A focus on South Korea. *Climate Dyn.*, **45**, 1699–1712, https://doi.org/10.1007/s00382-015-2546-9.

Kobayashi, S., and Coauthors, 2015: The JRA-55 reanalysis: General specifications and basic characteristics. *J. Meteor. Soc. Japan*, **93**, 5–48, https://doi.org/10.2151/jmsj.2015-001.

Lu, X., M. B. McElroy, and J. Kiviluoma, 2009: Global potential for wind-generated electricity. *Proc. Natl. Acad. Sci. USA*, **106**, 10 933–10 938, https://doi.org/10.1073/pnas.0904101106.

Marsh, P. T., H. E. Brooks, and D. J. Karoly, 2007: Assessment of the severe weather environment in North America simulated by a global climate model. *Atmos. Sci. Lett.*, **8**, 100–106, https://doi.org/10.1002/asl.159.

McVicar, T. R., T. G. Van Niel, L. T. Li, M. L. Roderick, D. P. Rayner, L. Ricciardulli, and R. J. Donohue, 2008: Wind speed climatology and trends for Australia, 1975–2006: Capturing the stilling phenomenon and comparison with near-surface reanalysis output. *Geophys. Res. Lett.*, **35**, L20403, https://doi.org/10.1029/2008GL035627.

——, and Coauthors, 2012: Global review and synthesis of trends in observed terrestrial near-surface wind speeds: Implications for evaporation. *J. Hydrol.*, **416–417**, 182–205, https://doi.org/10.1016/j.jhydrol.2011.10.024.

Menut, L., 2008: Sensitivity of hourly Saharan dust emissions to NCEP and ECMWF modeled wind speed. *J. Geophys. Res.*, **113**, D16201, https://doi.org/10.1029/2007JD009522.

Muggeo, V. M., 2003: Estimating regression models with unknown break-points. *Stat. Med.*, **22**, 3055–3071, https://doi.org/10.1002/sim.1545.

——, 2008: Segmented: An R package to fit regression models with broken-line relationships. *R News*, No. 8/1, R Foundation, Vienna, Austria, 20–25.

Pryor, S. C., and R. Barthelmie, 2010: Climate change impacts on wind energy: A review. *Renewable Sustainable Energy Rev.*, **14**, 430–437, https://doi.org/10.1016/j.rser.2009.07.028.

——, and Coauthors, 2009: Wind speed trends over the contiguous United States. *J. Geophys. Res.*, **114**, D14105, https://doi.org/10.1029/2008JD011416.

Ramon, J., L. Lledó, V. Torralba, A. Soret, and F. J. Doblas-Reyes, 2019: What global reanalysis best represents near-surface winds? *Quart. J. Roy. Meteor. Soc.*, **145**, 3236–3251, https://doi.org/10.1002/qj.3616.

Rehman, S., 2013: Long-term wind speed analysis and detection of its trends using Mann–Kendall test and linear regression method. *Arabian J. Sci. Eng.*, **38**, 421–437, https://doi.org/10.1007/s13369-012-0445-5.

Roderick, M. L., L. D. Rotstayn, G. D. Farquhar, and M. T. Hobbins, 2007: On the attribution of changing pan evaporation. *Geophys. Res. Lett.*, **34**, L17403, https://doi.org/10.1029/2007GL031166.

Rose, S., and J. Apt, 2016: Quantifying sources of uncertainty in reanalysis derived wind speed. *Renewable Energy*, **94**, 157–165, https://doi.org/10.1016/j.renene.2016.03.028.

Saha, S., and Coauthors, 2010: The NCEP Climate Forecast System Reanalysis. *Bull. Amer. Meteor. Soc.*, **91**, 1015–1058, https://doi.org/10.1175/2010BAMS3001.1.

——, and Coauthors, 2014: The NCEP Climate Forecast System version 2. *J. Climate*, **27**, 2185–2208, https://doi.org/10.1175/JCLI-D-12-00823.1.

Schäfer, B., C. Beck, K. Aihara, D. Witthaut, and M. Timme, 2018: Non-Gaussian power grid frequency fluctuations characterized by Lévy-stable laws and superstatistics. *Nat. Energy*, **3**, 119–126, https://doi.org/10.1038/s41560-017-0058-z.

Sheffield, J., G. Goteti, and E. F. Wood, 2006: Development of a 50-year high-resolution global dataset of meteorological forcings for land surface modeling. *J. Climate*, **19**, 3088–3111, https://doi.org/10.1175/JCLI3790.1.

Siam, M. S., M.-E. Demory, and E. A. Eltahir, 2013: Hydrological cycles over the Congo and Upper Blue Nile Basins: Evaluation of general circulation model simulations and reanalysis products. *J. Climate*, **26**, 8881–8894, https://doi.org/10.1175/JCLI-D-12-00404.1.

Smith, A., N. Lott, and R. Vose, 2011: The integrated surface database: Recent developments and partnerships. *Bull. Amer. Meteor. Soc.*, **92**, 704–708, https://doi.org/10.1175/2011BAMS3015.1.

Tian, Q., G. Huang, K. Hu, and D. Niyogi, 2019: Observed and global climate model based changes in wind power potential over the Northern Hemisphere during 1979–2016. *Energy*, **167**, 1224–1235, https://doi.org/10.1016/j.energy.2018.11.027.

Torralba, V., F. J. Doblas-Reyes, and N. Gonzalez-Reviriego, 2017: Uncertainty in recent near-surface wind speed trends: A global reanalysis intercomparison. *Environ. Res. Lett.*, **12**, 114019, https://doi.org/10.1088/1748-9326/aa8a58.

Troccoli, A., K. Muller, P. Coppin, R. Davy, C. Russell, and A. L. Hirsch, 2012: Long-term wind speed trends over Australia. *J. Climate*, **25**, 170–183, https://doi.org/10.1175/2011JCLI4198.1.

Vautard, R., J. Cattiaux, P. Yiou, J.-N. Thépaut, and P. Ciais, 2010: Northern Hemisphere atmospheric stilling partly attributed to an increase in surface roughness. *Nat. Geosci.*, **3**, 756–761, https://doi.org/10.1038/ngeo979.

Veers, P., and Coauthors, 2019: Grand challenges in the science of wind energy. *Science*, **366**, eaau2027, https://doi.org/10.1126/science.aau2027.

Wang, J., J. Hu, and K. Ma, 2016: Wind speed probability distribution estimation and wind energy assessment. *Renewable Sustainable Energy Rev.*, **60**, 881–899, https://doi.org/10.1016/j.rser.2016.01.057.

Wen, C., A. Kumar, and Y. Xue, 2019: Uncertainties in reanalysis surface wind stress and their relationship with observing systems. *Climate Dyn.*, **52**, 3061–3078, https://doi.org/10.1007/s00382-018-4310-4.

Wohland, J., N. E. Omrani, D. Witthaut, and N. S. Keenlyside, 2019: Inconsistent wind speed trends in current twentieth century reanalyses. *J. Geophys. Res. Atmos.*, **124**, 1931–1940, https://doi.org/10.1029/2018JD030083.

Wu, J., J. Zha, D. Zhao, and Q. Yang, 2018: Changes in terrestrial near-surface wind speed and their possible causes: An overview. *Climate Dyn.*, **51**, 2039–2078, https://doi.org/10.1007/s00382-017-3997-y.

Xue, Y., B. Huang, Z.-Z. Hu, A. Kumar, C. Wen, D. Behringer, and S. Nadiga, 2011: An assessment of oceanic variability in the NCEP Climate Forecast System Reanalysis. *Climate Dyn.*, **37**, 2511–2539, https://doi.org/10.1007/s00382-010-0954-4.

Zeng, Z., and Coauthors, 2018: Global terrestrial stilling: Does Earth's greening play a role? *Environ. Res. Lett.*, **13**, 124013, https://doi.org/10.1088/1748-9326/aaea84.

——, and Coauthors, 2019: A reversal in global terrestrial stilling and its implications for wind energy production. *Nat. Climate Change*, **9**, 979–985, https://doi.org/10.1038/s41558-019-0622-6.

Zha, J., J. Wu, D. Zhao, and J. Tang, 2019: A possible recovery of the near-surface wind speed in eastern China during winter after 2000 and the potential causes. *Theor. Appl. Climatol.*, **136**, 119–134, https://doi.org/10.1007/s00704-018-2471-z.